Large Fermi Density Waves on the Reconstructed Pt(100) Surface

C. S. Chang, W. B. Su, C. M. Wei, and Tien T. Tsong

Institute of Physics, Academia Sinica, Nankang, Taipei, Taiwan, Republic of China

Several long-range superstructures have been observed with the scanning tunneling microscopy on the reconstructed Pt(100) surface at room temperature. They are present in strained domains and involve both the Fermi electrons and the concomitant lattice distortions. A first-principles calculation shows that the top layer expanded $\sim 18\%$ on average and the Fermi surface for a single hexagon layer displays some nesting portions, which can be related to the wave vectors of the observed superstructures. Thus, these superstructures existing in the local domains of the reconstructed surface have the likely origin of incipent charge density waves.

PACS numbers: 68.35.Bs, 61.16.Ch, 68.35.Rh

The novel physical properties discovered in the systems of reduced dimensions have been one of the central issues of condensed matter physics in recent years [1]. Metal surfaces comprise a major portion of the two-dimensional (2D) systems under investigation; their structural and electronic properties are of fundamental importance in the surface-mediated dynamical and chemical processes, such as epitaxial growths and catalytic reactions. Since surface atoms have fewer neighbors, they usually relax and/or reconstruct to form localized electronic and atomic structures and thus often exhibit the low-dimensional characteristics [2,3]. For instance, the wavy nature of surface state electrons scattered by lattice steps [4], impurities, and quantum corrals [5] has been demonstrated with scanning tunneling microscopy (STM). In these observations, however, only free-electron-like surface electrons are involved. Recently, giant Friedel oscillations around some defects have been observed on the Be(0001) surface at low temperature [6]. The enhanced amplitude of the waves is attributed to the nearly perfect 2D nature of the surface; therefore, a many-body effect, either originated from an incipient charge density wave (CDW) [7] or the electron-phonon coupling [8,9], was able to stabilize the screening oscillations to a long range. Topics relevant to this line of study, for example, the phase transitions in two dimensions, are well documented and the driving origins of the transitions for various systems have been actively investigated [10,11]. Here, we report on a related phenomenon discovered on the reconstructed Pt(100) surface at *room temperature* using STM and *ab initio* calculations.

The reconstructed Pt(100) surfaces are prepared in ultra-high vacuum by a conventional method [12]. After the ion bombardment, the (1×1) surface transforms to a "quasi-hexagonal" phase upon annealing above 400 K and this "nonrotated" reconstruction is usually termed (5×20) or Pt(100)-hex. The reconstruction results in an excess of $\sim 20\%$ atomic density due to the formation of a top hexagon layer [Fig. 2(c) below] [13]. By further annealing to 1100 K, the surface then changes to a "rotated" hexagonal phase, usually called Pt(100)-hex-0.7° [12–15]. These

structural phase transformations are irreversible, indicating that the small rotation is invoked to minimize the misfit energy between the hexagon layer and the square substrate. The resulting surface is buckled and characterized with the reconstruction lines (RL's) as a set of rows running diagonally from upper left to lower right in Fig. 1. Brighter areas in an STM image normally represent regions of higher electronic state density.
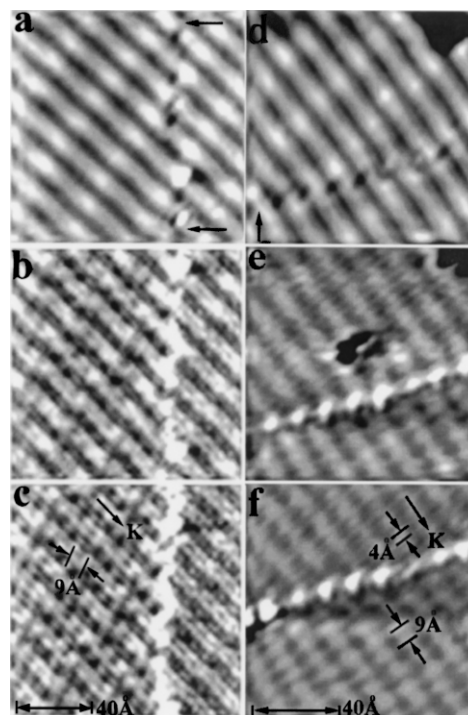

FIG. 1. Superstructures found on the reconstructed Pt(100) surface near a boundary (indicated by the arrows). (a)–(c): The amplitude of the superstructures as function of biases; (a) -0.1 V, no superstructures; (b) -0.03 V, superstructures appearing; (c) -0.01 V, superstructures with large amplitude. (d)–(f): The effect of creating a hole near the boundary; (d) before the hole creation; (e) 20 s and (f) 280 s after the hole creation (see text). Superstructures of different wavelengths are marked and the $\Gamma\mathbf{K}$ direction in the reciprocal lattice is indicated by an arrow ending with $\mathbf{K}$.

Figures 1(a)–1(c) show the reconstructed Pt(100) surface near a pinned domain boundary as a function of the tunneling bias. When the bias is −0.1 V, only the reconstruction lines and a dim rotational boundary are seen [Fig. 1(a)]. The superstructures are clearly visible as the bias decreases to −0.03 V [Fig. 1(b)]. Their amplitude becomes larger at the bias of −0.01 V [Fig. 1(c)]. This indicates that the superstructures are originated from the electronic states near the Fermi surface and their amplitude apparently corresponds to the density of electronic states at the boundary, which also gets higher closer to the Fermi level.

Similar superstructures can also be found if a hole is artificially created near a boundary [Fig. 1(e)] with a high voltage pulse [16]. Before the hole is created, the boundary appears dim, possibly a result of the partial stress relief [Fig. 1(d)]. The local lattice responded with a dramatic change at the boundary to the existence of the hole. The original dim boundary turns to a bright one. At the same time, new superstructures appear on both sides of the boundary, where either the excess strain or charge is accumulated. These new periodic structures are apparently pinned by the bright boundary [Fig. 1(f)] and do not fade away from it within the imaged range. This excited state due to the perturbation is metastable at room temperature, and can only last for a few minutes before it returns back to the original structure of Fig. 1(d), when the hole is self-repaired by surface diffusion.

The superstructures shown in Fig. 1 have rather short wavelengths of ∼4 and ∼9 Å and appear as stripes nearly perpendicular to the RL's [Figs. 1(c) and 1(f)]. They arise in order to correspond with the bright feature at a structural domain boundary and exhibit a long-range periodic character at room temperature. The bright feature at the boundary is attributed to an excess of electronic states close to the Fermi surface [Fig. 1(b)], which can also be induced with a local strain field [Fig. 1(e)]. These results combine to suggest a coupling between the Fermi electrons and the lattice deformation mediated through a boundary, which is a many-body effect [6]. The boundary seems to possess a great capacity for the excess stress and charge, and thus facilitates the coupling in the delineated domain. An intriguing issue here is what drives this phenomenon to occur, which calls for further examination in more detail of how the superstructures are related to the reconstructed structure.

Figure 2 shows an atomically resolved STM image of the incommensurate Pt(100)-hex surface exhibiting similar superstructures to those in Fig. 1. This image is taken in a narrow terrace and the atomic lattice is likely to be deformed. The surface thus exhibits a slightly different reconstruction involving a larger top-layer rotation. It could be for this reason that the picture displays a three-phase superstructure in addition to the atomic structure [Fig. 2(a)]. The accompanying atomic structure is always helpful in analyzing the direction and wavelength of the
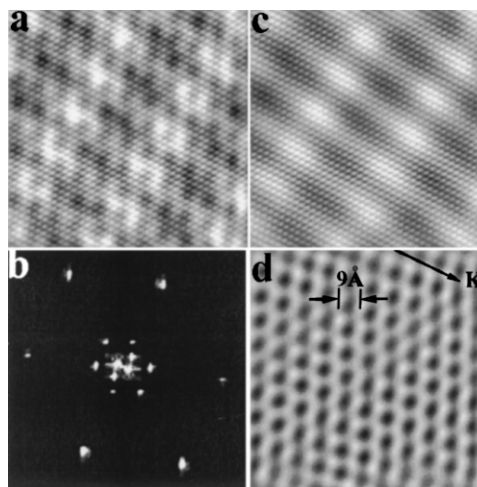

FIG. 2.   A 100 Å × 100 Å STM image taken in a narrow terrace on the Pt(100) surface showing (a) the atomic structure mixed with a superstructure, (b) Fourier transform pattern of this image, (c) the atomically resolved reconstruction, and (d) the quasihexagonal superstructure.

superstructure, especially in the Fourier space [as shown in Fig. 2(b)]. The six spots arranged in a hexagon near the origin are due to the superstructure. This can be confirmed by performing a backtransformation of the Fourier pattern with just the inner six spots selected, as illustrated in Fig. 2(d). Other spots thus pertain to the geometrical arrangement of the surface atoms [Fig. 2(c)]. As for the superstructure, since only the top layer has the hexagonal symmetry, it is natural to attribute its origin to the top layer. This superstructure has a wavelength of ∼9 Å and appears only when the bias is within a narrow range (usually <0.1 V) of the Fermi level. Further inspection of Fig. 2(b) indicates that the superstructure is incommensurate with the substrate lattice. The ratio in unit length between the superstructure and the atomic lattice is ∼3.5 and the angle between them is ∼5°.

Because of the large discrepancy in atomic arrangements and bond lengths of the surface and substrate, surface atoms in both rotated and nonrotated phases seem to bond much more strongly within the top hexagon layer than with those in the underneath substrate. Its "quasi-2D" character can be inferred from the experimental fact that the top layer, at least in one direction, is only weakly coupled to the substrate [12], and has indeed been verified by our *ab initio* calculations. Our calculations, based on the local density approximation [17], were done for the (5 × 1) reconstruction simply because the true unit mesh is too large. It was performed using the efficient and accurate total-energy and molecular-dynamics package—VASP (Vienna *ab initio* simulation package) [18–20]. The (5 × 1) surface is simulated by five-layer slabs and separated by six layers of vacuum. The **k** points were summed over a (6 × 30) Monkhorst-Pack grid with 45 points in the (5 × 1) irreducible part of the surface Brillouin zone. To start the simulation, we placed six surface atoms, with the

structure inferred by LEED data [13], on top of five substrate atoms in a $\langle 110 \rangle$ direction on the (100) surface. The bottom two layers were fixed and the top three were free to relax [21].

The fully relaxed final structure of the calculation has indeed a lower energy of 0.35 eV/[(5×1) unit cell] than the (1×1) surface. It also exhibits a surface corrugation of ~ 0.4 Å, in close agreement with experiment [13], and a 2.9% reduction of bond length in the top layer as shown in Fig. 3(a). Since the Pt bonding involves a great amount of d electrons, the decrease of the bond length will enhance a much stronger interaction within the top layer. The spacing between the first and second layers is further found to be expanded $\sim 18\%$ on average [Fig. 3(a)], indicating a weakening of interlayer interaction. Because of this large interaction anisotropy, the top hexagon layer should possess rather unique properties for its electrons and phonons. In an approximation, these top-layer properties may then be treated first, and the substrate effects can be considered later as a perturbation. To explore the possible 2D character inherent to this system, we calculated the Fermi surface for a perfect Pt hexagon layer with a bond length of 2.67 Å and plotted the results in the first Brillouin zone [Fig. 3(b)]. In this diagram, the Fermi surface of sixfold symmetry is multicontoured with two electron lines (solid curves) and two hole lines (dotted curves). Between these lines, several parallel segments for possible nesting exist and some of them along the ΓK and ΓM directions are indicated with the vectors $\mathbf{a}$, $\mathbf{b}$, $\mathbf{c}$, etc. The ΓK direction is indicated by an arrow ending with $\mathbf{K}$ in each figure displaying a superstructure. If all of the observed superstructures could be associated with the nesting vectors on the Fermi lines, it would be very convincing evidence for their origin of electronic instability. As the first example, the nesting vectors marked $\mathbf{a}$, $\mathbf{a}'$ and $\mathbf{a}''$ can be implemented to generate three sinusoidal waves, which can form a pattern [Fig. 3(c)] resembling the superstructure shown in Fig. 2(d). The

superstructures with a wavelength of 4 Å in Fig. 1 can be associated with the nesting vector $\mathbf{d}$.

Figure 4 presents yet two other superstructures observed on this surface. In the images with mixed geometric and super structures [Figs. 4(a) and 4(c)], the amplitude of the latter is apparently dominant. The three-phase incommensurate waves in Fig. 4(a) are so outstanding that the buckled surface is hardly recognizable. After separating the atomic structures from the figures, the superstructures once again display a nearly hexagonal symmetry, as shown in Figs. 4(b) and 4(d). Referring their wavelengths and directions to the atomic structures, we can attribute the formation of the superstructure with a wavelength of ~ 13 Å [Fig. 4(b)] to the vector marked $\mathbf{b}$, and that of ~ 28 Å [Fig. 4(d)] to $\mathbf{c}$ in the Fermi diagram [Fig. 3(b)].

At this point, we are very much convinced that a superstructure occurs through an electron-phonon coupling made easier by several factors. The 2D character of the top hexagon layer defines the possibility of nesting in the Fermi lines. These Fermi lines are sensitively related to the arrangement of surface Pt atoms. The incommensurate nature of the reconstructed surface renders many possible rotational and compressible states associated with the local environment. Finally, domain boundaries and artificially created defects are usually involved as a fine-tuned parameter for the Fermi electrons to couple with the lattice.

Although the superstructures observed here seem to be a local phenomenon, their implication to the phase transformation could be very profound. It is known that in the first-order phase transition, as for the "nonrotated to rotated" phase transformation here, the process usually involves nucleation and growth. The nucleation could start from some defect sites on the surface, where the steps, vacancies, and impurities are located. These imperfections are ubiquitous for the solid surfaces and could pin the growth of a certain phase. Thus, locally, the superstructure states can be quite stable. With the help of defects, the
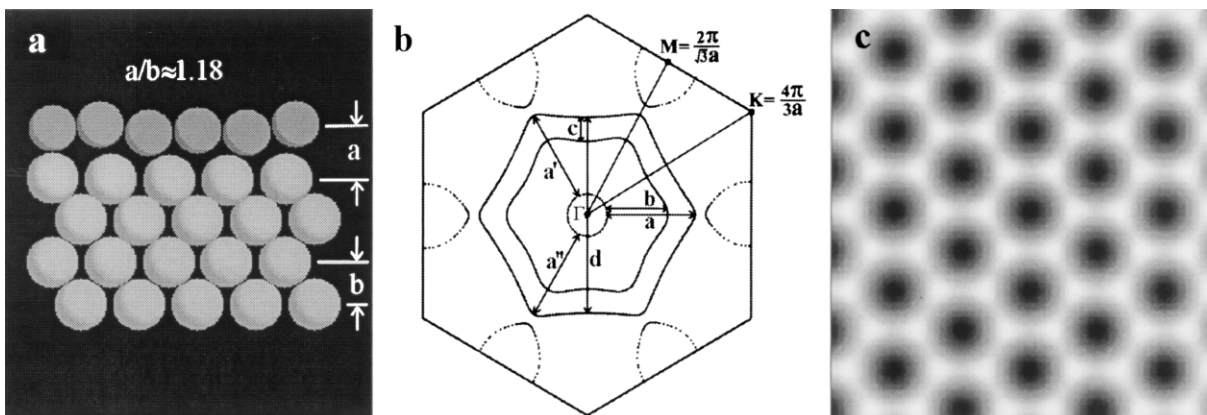

FIG. 3. (a) Side view of the calculated (5×1) reconstruction after the relaxation; (b) calculated Fermi lines for a single Pt hexagon layer, the vectors $\mathbf{a}$, $\mathbf{b}$, $\mathbf{c}$, $\mathbf{d}$ connecting the possible nesting portions between the lines; (c) computer simulated pattern in gray-scale presentation using the three vectors indicated in (b) (see text).
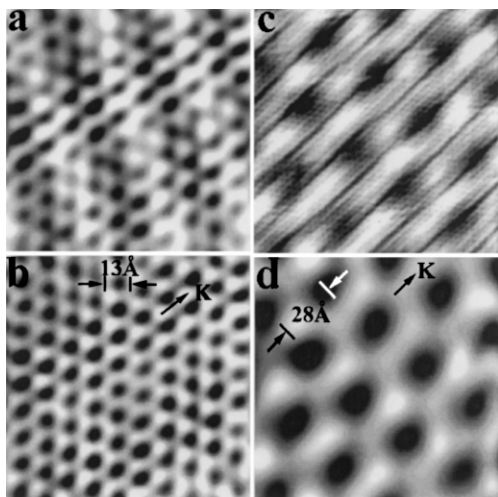
FIG. 4.   Two more superstructures found on the reconstructed Pt(100) surface. (a) A 120 Å × 120 Å STM image of the reconstruction mixed with a dominant superstructure, (b) the quasihexagonal superstructure of (a), (c) a 115 Å × 115 Å STM image of the atomically resolved reconstruction and a superstructure, and (d) the quasihexagonal superstructure of (c).

system could be locked into a state with the coexistence of many regional domains defined by different superstructures. Such a state has indeed been found on the reconstructed Pt(100) surface [22]. It is hence plausible that this CDW instability might play some role in the reconstruction of the Pt(100) surface as well.

[1] *Highlights in Condensed Matter Physics and Future Prospects,* edited by L. Esaki, NATO ASI Series (Plenum Press, New York, 1991); *Interacting Electrons in Reduced Dimensions,* edited by D. Baeriswyl and D. K. Campbell (Plenum Press, New York, 1989).

[2] A. Zangwill, *Physics at Surfaces* (Cambridge University Press, Cambridge, England, 1988), Chaps. 3 and 4.

[3] C. S. Chang, W. B. Su, and T. T. Tsong, Jpn. J. Appl. Phys. **34**, 3329 (1995).

[4] Y. Hasegawa and Ph. Avouris, Phys. Rev. Lett. **71**, 1071 (1993); Ph. Avouris and I.-W. Lyo, Science **264**, 942 (1994).

[5] M. F. Crommie, C. P. Lutz, and D. M. Eigler, Nature (London) **363**, 524 (1993); Science **262**, 218 (1993).

[6] P. T. Sprunger, L. Petersen, E. W. Plummer, E. Lægsgaard, and F. Besenbacher, Science **275**, 1764 (1997); Ph. Hofman, B. G. Briner, M. Doering, H.-P. Rust, E. W. Plummer, and A. M. Bradshaw, Phys. Rev. Lett. **79**, 265 (1997).

[7] R. E. Peierls, *Quantum Theory of Solids* (Oxford University Press, Oxford, 1955); A. W. Overhauser, Phys. Rev. B **2**, 874 (1970).

[8] N. W. Ashcroft and N. D. Mermin, *Solid State Physics* (Holt, Rinehart and Winston, New York, 1976), Chap. 26.

[9] J. Friedel, in *Electron-Phonon Interactions and Phase Transitions,* edited by T. Riste, NATO ASI Series (Plenum Press, New York, 1977); A. Fasolino, G. Santoro, and E. Tosatti, Surf. Sci. **125**, 317 (1983).

[10] R. F. Willis, in *Dynamical Phenomena at Surfaces, Interfaces and Superstructures,* edited by F. Nizzoli, K. H. Rieder, and R. F. Willis (Springer, Berlin, 1985).

[11] J. M. Carpinelli, H. H. Weitering, E. W. Plummer, and R. Stumpf, Nature (London) **381**, 398 (1996); A. Mascaraque, J. Avila, J. Alvarez, M. C. Asensio, S. Ferrer, and E. G. Michel, Phys. Rev. Lett. **82**, 2524 (1999).

[12] M. A. Van Hove, R. J. Koestner, P. C. Stair, J. P. Biberian, L. L. Kesmodel, I. Bartos, and G. A. Somorjai, Surf. Sci. **103**, 189 (1981).

[13] A. Borg, A. M. Hilmen, and E. Bergene, Surf. Sci. **306**, 10 (1994); G. Ritz, M. Schmid, P. Varga, A. Borg, and M. Rønning, Phys. Rev. B **56**, 10 518 (1997).

[14] N. Bickel and K. Heinz, Surf. Sci. **163**, 453 (1985).

[15] V. Fiorentini, M. Methfessel, and M. Schleffler, Phys. Rev. Lett. **71**, 1051 (1993).

[16] C. S. Chang, W. B. Su, and Tien T. Tsong, Phys. Rev. Lett. **72**, 574 (1994).

[17] *The Theory of the Inhomogeneous Electron Gas,* edited by S. Lundqvist and N. H. March (Plenum, New York, 1983); W. E. Pickett, Comput. Phys. Rep. **9**, 115 (1989).

[18] G. Kresse and J. Hafner, Phys. Rev. B **47**, 558 (1993); **49**, 14 251 (1994).

[19] G. Kresse and J. Furthmüller, Comput. Mater. Sci. **6**, 15 (1996).

[20] G. Kresse and J. Furthmüller, Phys. Rev. B **54**, 11 169 (1996).

[21] An ultrasoft Pt pseudopotential with a 14 Ry energy cutoff was employed to ensure absolute convergence of total energies to ~ 10 meV. To accelerate the electronic relaxation, we use the Fermi-smearing method with a width of 0.01 eV.

[22] C. S. Chang, W. B. Su, C. M. Wei, and T. T. Tsong (to be published).